Analysis of Ridge-Loaded Folded-Waveguide Slow-Wave Structures for Broadband Traveling-Wave Tubes

M. Sumathy, K. J. Vinoy, *Member, IEEE*, and S. K. Datta, *Member, IEEE*

***Abstract*—An E-plane serpentine folded-waveguide slow-wave structure with ridge loading on one of its broad walls is proposed for broadband traveling-wave tubes (TWTs) and studied using a simple quasi-transverse-electromagnetic analysis for the dispersion and interaction impedance characteristics, including the effects of the beam-hole discontinuity. The results are validated against cold test measurements, an approximate transmission-line parametric analysis, an equivalent circuit analysis, and 3-D electromagnetic modeling using CST Microwave Studio. The effect of the structure parameters on widening the bandwidth of a TWT is also studied.**

***Index Terms*—Broadbanding, equivalent circuit analysis, folded-waveguide slow-wave structure (SWS), quasi-transverse-electromagnetic (quasi-TEM) analysis, ridge loading.**

I. Introduction

SERPENTINE folded-waveguide slow-wave structures (SWSs) enjoy several advantages over their counterparts in the millimeter-wave frequency range, including robust construction, high-power handling capability, wideband potential, and ease of fabrication. Consequently, there is great interest in the study and development of high-power millimeter-wave folded-waveguide traveling-wave tubes (TWTs) [1]–[7]. Analysis leading to the dispersion and interaction impedance characteristics of the structure includes the transmission-line parametric modeling [2]–[6], equivalent circuit analysis [5]–[7], and 3-D electromagnetic modeling [6], [7]. Some work has also been reported on ridge-loaded folded-waveguide SWSs for their wideband potential, for instance, [8] and [9] for E-plane-bend and H-plane-bend structures, respectively.

In this paper, we propose ridge loading on one of the broad walls of the rectangular waveguide (Fig. 1), with an aim to study the effect of the ridge width and the ridge height on enhancing the bandwidth of the device. To analyse the proposed model, we introduce a simple quasi-transverse-electromagnetic (quasi-TEM) approach [10]–[14], which results in a closed-form solution for dispersion and interaction impedance.

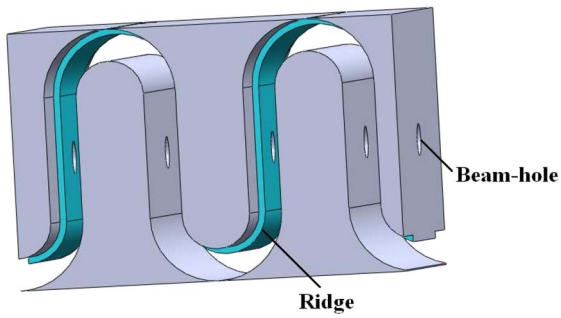

Fig. 1. Schematic of an E-plane serpentine folded waveguide with ridge loading on one of its broad walls.

The classical method of quasi-TEM analysis for a waveguide-derived SWS (Section II) was carried out by Fletcher for a broadband interdigital circuit [10] that comprises the analysis of an iterative circuit composed of a pair of lines: a transverse-electromagnetic (TEM) line and a waveguide section. The approach was extended for different variants of interdigital SWSs by Walling [11], Paschke [12], and Hirano [13], [14], providing a convenient method for incorporating the discontinuities in the structure through a "discontinuity function." However, to the best of our knowledge, a quasi-TEM analysis has not been used so far for analyzing a folded-waveguide SWS. The present quasi-TEM analysis is simpler than the other approaches and is easily extended to a complex ridge-loaded folded-waveguide SWS, including taking into account the effect of the discontinuities at the E-bend and beam holes. Moreover, the present analysis also provides closed-form expressions for the characterization of the structure with respect to the dispersion and the interaction impedance of the structure. We have also performed an approximate transmission-line parametric analysis (Appendix A), which, unlike the quasi-TEM analysis, does not include the effects of bend and hole discontinuities.

The present analysis proceeds in the following steps in Section II. First, we model the straight waveguide section of the SWS supporting the TE_{10} mode as a TEM line (Fig. 2); next, we incorporate the effect of the discontinuities due to the E-plane-bend section and the beam hole in the structure through a "discontinuity function" in the derivation of the SWS phase velocity dispersion. We then carry out the analysis for the interaction impedance of the structure including the

Manuscript received November 11, 2009; revised February 22, 2010; accepted March 2, 2010. Date of publication April 15, 2010; date of current version May 19, 2010. The review of this paper was arranged by Editor W. Menninger.

M. Sumathy is with the Microwave Tube Research and Development Centre, Defence Research and Development Organization, Bangalore 560 013, India, and also with the Indian Institute of Science, Bangalore 560054, India (e-mail: msumti@yahoo.co.in).

K. J. Vinoy is with the Department of Electronics and Communication Engineering, Indian Institute of Science, Bangalore 560054, India.

S. K. Datta is with the Microwave Tube Research and Development Centre, Defence Research and Development Organization, Bangalore 560 013, India.

Color versions of one or more of the figures in this paper are available online at http://ieeexplore.ieee.org.

Digital Object Identifier 10.1109/TED.2010.2045680

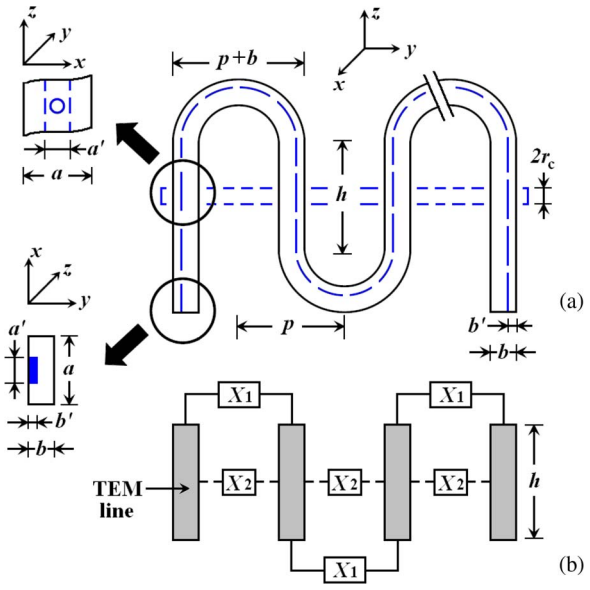

Fig. 2. (a) Schematic of a typical ridge-loaded serpentine folded-waveguide SWS. (b) Its equivalent quasi-TEM circuit representation including the discontinuities due to the waveguide bend (X_1) and the beam hole (X_2).

effects of the gap field and space-harmonic effects following the parametric approach used by Hutter [15], Liu [2], and Booske *et al.* [6]. In Section III, the analysis is validated against cold test measurements and full 3-D simulation using CST Microwave Studio (following Booske *et al.* [6]), as well as against the parametric and the equivalent circuit approaches of Booske *et al.* [6] and Sumathy *et al.* [7], respectively. Finally, the analysis is used to study the control of the SWS dispersion by ridge loading for broadband TWTs.

II. Analysis

A waveguide-based structure lends itself to quasi-TEM modeling under the following conditions [10]–[14], [16]–[20].

1) $b \ll a$ and $b \ll \lambda_g$, with a being the waveguide broad-wall width, b being the waveguide narrow-wall height, and λ_g being the guide wavelength.
2) The electric field component along the direction of propagation $\ll$ the electric field component transverse to the direction of propagation.

Under such conditions, the propagation behavior of the structure may be described under quasi-static conditions that result in approximately static field solutions obeying Laplace's equation rather than Helmholtz's equation [16]–[23]. This allows an equivalent circuit analysis of the structure using lumped circuit parameters. This approximation provides reasonably accurate results when $b < 0.2\lambda_g$ [18], a condition that encompasses a wide range of ridge-loaded waveguide structures [21]–[23].

Subject to the above two conditions, a folded-waveguide SWS (typically with $b/a \sim 0.1$) formed by a dominant-mode ridge-loaded rectangular waveguide is configured in a quasi-TEM model (Fig. 2). The folded waveguide (broad-wall width $= a$, and narrow-wall height $= b$) considered for the present analysis is of periodicity $= p$, ridge width $= a'$, and ridge height $= b'$. Each period of the folded-waveguide SWS consists of two waveguide elements: 1) a straight ridge-loaded waveguide section of length h treated as a TEM line (TEM-like-wave propagation considered to be in the z-direction) accommodating the beam holes (each of radius r_c) as apertures at the broad waveguide walls and 2) an E-plane ridge-loaded waveguide-bend section of mean bending radius R_b $(= p/2)$ and axial width d $(= p + b)$ with an equivalent discontinuity reactance X_1 (Fig. 2). The beam hole has an equivalent discontinuity reactance X_2 (Fig. 2).

The field in the TEM line is described in terms of TEM-like waves traveling along the z-direction. The voltage at the mth TEM line may be expressed following Fletcher [10], Walling [11], and Hirano [13], [14] in the form

$$V_m\{z\} = A_1 \cos\{k_z z\} e^{-jm(\phi+\pi)} + A_2 \sin\{k_z z\}^{-jm\phi}. \quad (1)$$

Here, A_1 and A_2 are field constants, ϕ is the phase shift per period for the fundamental space-harmonic wave, k_z $(= (2\pi/\lambda_g)(1 + p/h))$ is the effective z-directed propagation constant of the TEM line [12]–[14], and λ_g is the guide wavelength. Here, ϕ is related to the effective axial phase shift of the fundamental space-harmonic wave of the SWS (β_0) by $\beta_0\, p = \phi + \pi$.

Considering the circuit to be lossless, we define the gap voltage at the location of the electron beam axis, in view of the periodicity of the structure, as [10]–[14]

$$V_m\{h/2\} = -V_{m+1}\{h/2\}$$

which, with the help of (1), yields

$$j(A_1/A_2) = \tan\left\{\frac{1}{2}k_z h\right\} \cot\{\phi/2\}. \quad (2)$$

Following the quasi-TEM approach proposed by Walling [10], Paschke [11], and Hirano [12], [13], we eliminate the field constants in (2) using a discontinuity function z_i defined as

$$j(A_1/A_2) = \tan\left\{\frac{1}{2}k_z h\right\} \cot\{\phi/2\} = z_i \quad (3)$$

which is then expressed by cascading the discontinuity reactances due to the waveguide bend (X_1) and the beam hole (X_2) to the TEM line in the form [12]–[14]

$$z_i = \sqrt{\left(\frac{1 - \frac{1}{2}\left(\frac{Z_0}{X_1+X_2}\right)\tan\left\{\frac{1}{2}k_z h\right\}}{1 + \frac{1}{2}\left(\frac{Z_0}{X_1+X_2}\right)\cot\left\{\frac{1}{2}k_z h\right\}}\right)}. \quad (4)$$

Here, Z_0 $(\approx 120\pi b_1/h)$ is the characteristic impedance of the TEM line, and b_1 $(= b - b')$ is the transverse narrow-wall height of the ridge-loaded waveguide.

The transition from a straight waveguide to a smooth circular E-bend has a slightly higher characteristic impedance than the straight portion, and there exists a capacitive susceptance at the transition [16], [17]. In the case of a folded-waveguide SWS, the radius of curvature of the bend is usually large enough to keep the TE_{10} mode transition unaffected without exciting unwanted evanescent modes, allowing the capacitive susceptance to be ignored at the transition region. However, the bending of the transverse electric field lines causes a slight

change in the guide wavelength in the bend region, which changes the characteristic impedance of the waveguide bend. This change is governed by the bending radius (R_b) and the waveguide narrow-wall height (b_1) and is approximated using the variational expression of Marcuvitz [16] applicable within the regime $2b_1/\lambda_g < 1$. An exact expression for the change in the characteristic impedance due to the bend is available in [16] for the case of an ordinary ridge-free waveguide ($b_1 = b$, with $b' = 0$). For the case of a ridge-loaded waveguide, we have heuristically applied here the same expression with the restrictions imposed that no higher mode interaction exists between the ridge and the narrow-wall of the guide, which is approximately the case if $(a - a')/2b_1 \gg 1$ for the dominant propagating mode [16]. The present heuristic approach stems from the concept that, in the absence of higher order modes, the equivalent circuit model is described by a scalar potential $(V_{\rm gap} = E_{\rm gap} b_1)$ defined as the product of the electric field between the broad walls $(E_{\rm gap})$ and the gap between the broad walls (b_1). Thus, following the equivalent circuit analysis of Marcuvitz [16], the discontinuity reactance due to the E-bend serpentine section may approximately be expressed as

$$X_1 \approx Z_{VI}\left[1+\frac{1}{24}\left(\frac{b_1}{R_b}\right)^2-\frac{1}{60}\left(\frac{b_1}{R_b}\right)^2\left(\frac{2\pi b_1}{\lambda_g}\right)^2\right]. \quad (5)$$

Here, Z_{VI} is the voltage–current characteristic impedance of the ridge-loaded waveguide. Again, for the $\rm TE_{10}$ mode of propagation: 1) both ordinary and ridge-loaded waveguides would possess a sinusoidal distribution of transverse electric field normal to the broad wall of the guide with a maximum amplitude at the center of the broad wall and 2) a small aperture $(r_c \ll \lambda_g, r_c \ll a')$ at the location of the electric field maximum would show the same electric polarizability $(\alpha_e = -2r_c^3/3)$ and magnetic polarizability $(\alpha_m = 4r_c^3/3)$ for both types of waveguides. Assuming no higher mode interaction between the ridge and the narrow wall of the guide (which is approximately the case if $(a - a')/2b_1 \gg 1$ [16]), one may directly follow the derivation in [20] for a conventional unfolded and ridge-free rectangular waveguide to write the susceptance of the beam hole (X_2) as

$$X_2 = \frac{32\pi r_c^3 Z_{VI}}{3\lambda_g a b_1}. \quad (6)$$

Furthermore, the voltage–current characteristic impedance (Z_{VI}) of the ridge-loaded waveguide used in (5) and (6) may be expressed as [21]–[23]

$$Z_{VI} = \frac{120\pi^2(b-b')(\lambda_g/\lambda)}{\lambda_c\left[\sin\{\theta_2\}+\left(\frac{b-b'}{b}\right)\cos\{\theta_2\}\tan\{\theta_1/2\}\right]} \quad (7)$$

where $\theta_1 = \pi(a - a')/\lambda_c$, and $\theta_2 = \pi(a'/\lambda_c)$. λ is the free-space wavelength, and λ_c is the cutoff wavelength of the ridge-loaded waveguide.

The dispersion relation of the folded-waveguide SWS is now expressed, with the help of (3)–(7), as

$$\beta_0 = \frac{\pi}{p} + \frac{2}{p}\tan^{-1}\left\{\frac{1}{z_i}\tan\left\{\frac{1}{2}k_z h\right\}\right\} \quad (8)$$

which is then used to compute the axial RF phase velocity v_p $(= 2\pi f/\beta_0)$ at the operating frequency (f).

The on-axis interaction impedance of the structure is obtained from the following expression [2], [6], [15]:

$$K_c = Z_{PV}\left(\frac{1}{(\beta_0 p)}\left(\frac{\sin\left\{\beta_0\left(\frac{b-b'}{2}\right)\right\}}{\beta_0\left(\frac{b-b'}{2}\right)}\right)\right)^2 \quad (9)$$

where Z_{PV} $(= 2Z_{VI}/\pi)$ is the power–voltage characteristic impedance of the waveguide. Using (8) and (9), one obtains the dispersion and interaction impedance characteristics, respectively, of the ridge-loaded folded-waveguide SWS.

A figure of merit of the ridge-loaded folded-waveguide SWS with reference to a TWT is the well-known Pierce's normalized circuit gain parameter [15], [24], i.e.,

$$CN = \left(\frac{K_c I_0}{4V_0}\right)^{\frac{1}{3}}\left(\frac{\omega l_{ckt}}{2\pi u_0}\right) \quad (10)$$

where $C(= (K_c I_0/4V_0)^{1/3})$ is Pierce's gain parameter [24], and $N(= \omega l_{\rm ckt}/(2\pi u_0))$ is the normalized interaction length [24]. I_0 and V_0 are the beam current and the beam voltage, respectively; u_0 is the unperturbed velocity of the electron beam; and $l_{\rm ckt}$ is the axial interaction length.

III. Results and Discussion

To validate the present quasi-TEM analysis, we consider two typical serpentine folded-waveguide SWSs, one of which operates in the Ka-band and the other in the W-band. The validation is carried out for the special case of $a'/a = 1.0$ and $b'/b = 0.0$, which reduces the structure to the conventional serpentine folded-waveguide SWS without ridge loading. The validation of the present quasi-TEM analysis with respect to the Ka-band structure is done against measurements [7], the equivalent circuit analysis, the 3-D CST Microwave Studio simulation, and the parametric analysis (Fig. 3). The validation of the present analysis with respect to the W-band structure is done against the equivalent circuit analysis, the 3-D CST Microwave Studio simulation, and the parametric analysis (Fig. 4). The 3-D simulation using CST Microwave Studio was carried out following the approach of Booske *et al.* [6], using the eigenmode solver and modeling two periods of the structure. As shown in Fig. 3, the present quasi-TEM analysis shows approximately 1% deviation against the measurement and approximately 2% deviation against the CST Microwave Studio simulation, over 28–36 GHz, with respect to the dispersion characteristics for the Ka-band structure. For the W-band structure dispersion characteristics, shown in Fig. 4, over 85–115 GHz, the present analysis deviates by 2% from the CST Microwave Studio simulation. For dispersion characteristics, the present analysis agrees more closely with both the CST Microwave Studio simulation and the experiment than with the approximate transmission-line parametric analysis (ignoring the effects of discontinuities due to the E-bend and the beam holes). Note that the parametric analysis works well for the prediction of interaction impedance.

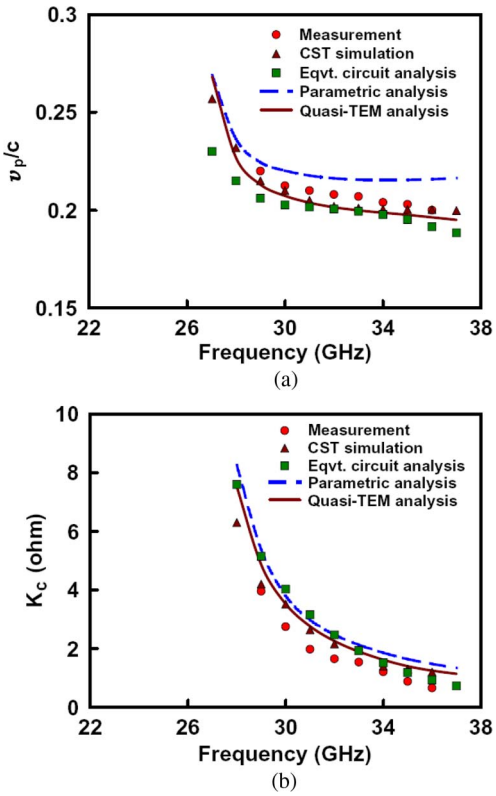

Fig. 3. (a) Dispersion and (b) interaction impedance characteristics of a Ka-band serpentine folded-waveguide SWS, with $a'/a = 1$ and $b'/b = 0$, obtained by various analyses and by measurement ($f_\pi = 27.03$ GHz).

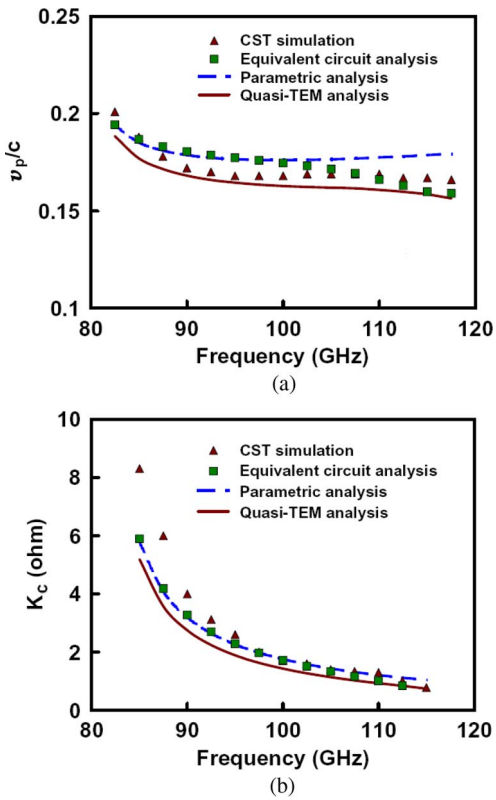

Fig. 4. (a) Dispersion and (b) interaction impedance characteristics of a W-band serpentine folded-waveguide SWS, with $a'/a = 1$ and $b'/b = 0$, obtained by various analyses ($f_\pi = 81.08$ GHz).

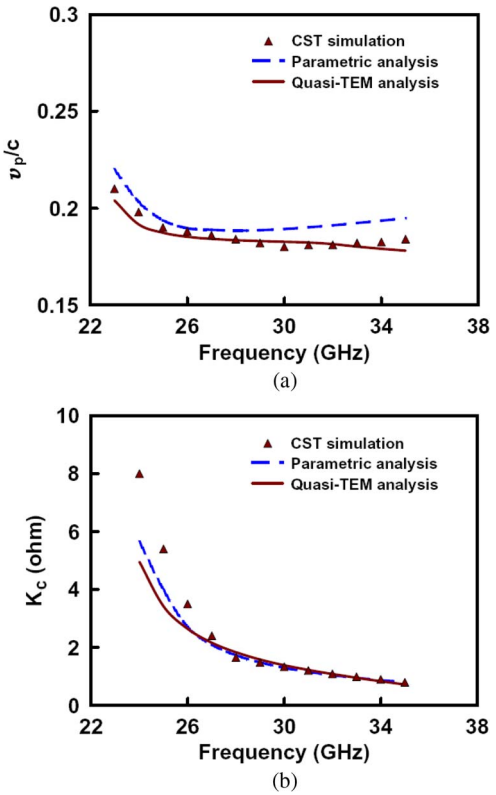

Fig. 5. (a) Dispersion and (b) interaction impedance characteristics of a Ka-band ridge-loaded serpentine folded-waveguide SWS, with $a'/a = 0.5$ and $b'/b = 0.2$, obtained by various analyses ($f_\pi = 22.52$ GHz).

We now use a Ka-band structure to demonstrate the efficacy of a ridge-loaded SWS. As shown in Fig. 5, the dispersion characteristics of the ridge-loaded structure obtained by the present quasi-TEM approach agree well with the 3-D CST Microwave Studio simulation; however, all the analytical predictions of the interaction impedance characteristics show noticeable deviations against the CST Microwave Studio simulation around the frequency regime corresponding to the phase shift per period close to π. This may be attributed to the limitations of analytical approaches to correctly predict the waveguide impedance around the cutoff frequency where the group velocity of the wave approaches zero.

The π-mode and 2π-mode cutoff frequencies of the ridge-loaded SWS, i.e., f_π and $f_{2\pi}$, respectively, for different combinations of the normalized ridge width (a'/a) and the normalized ridge height (b'/b) are shown in Fig. 6 (predicted by CST Microwave Studio). The ridge loading reduces both f_π and $f_{2\pi}$. The reduction in f_π is relatively larger than that in $f_{2\pi}$, accommodating an effective increase in the cold bandwidth. Suitable control of the ridge width and the ridge height enables improving the dispersion characteristics from positive dispersion (phase velocity decreasing with frequency) to flat dispersion over a broader range of frequencies [Fig. 7(a)] suitable for broadband operation. However, for ensuring broadband operation, one needs to analyze the effect of the reduction in interaction impedance across frequency. This necessitates evaluation of the frequency response of Pierce's normalized circuit gain (CN). Fig. 8 shows a comparison of CN versus frequency for different combinations of the normalized ridge

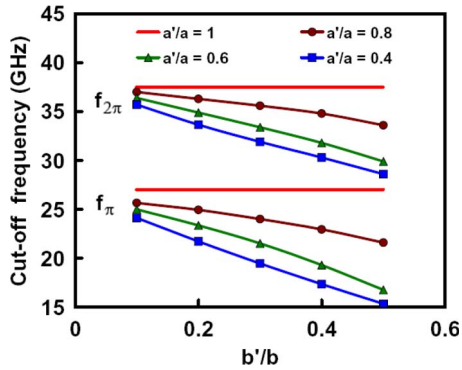

Fig. 6. Comparison of f_π and $f_{2\pi}$ of the Ka-band ridge-loaded SWS for different values of the normalized ridge width (a'/a) and the normalized ridge height (b'/b).

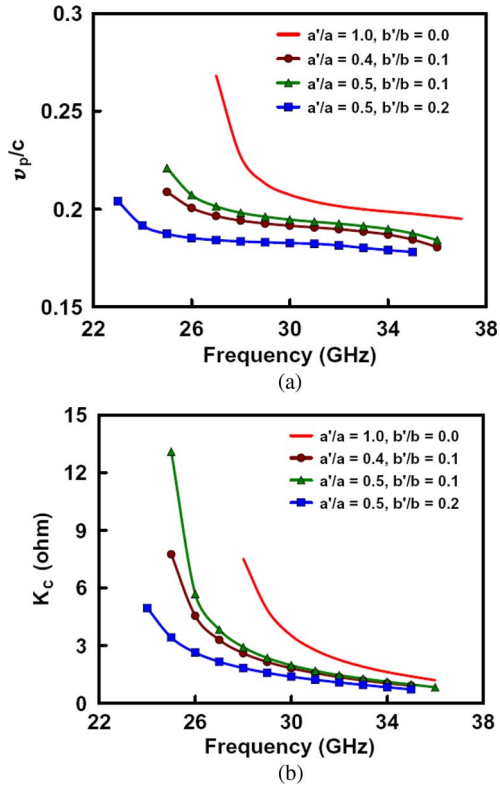

Fig. 7. (a) Dispersion and (b) interaction impedance characteristics of the Ka-band ridge-loaded serpentine folded-waveguide SWS for different combinations of the normalized ridge width (a'/a) and the normalized ridge height (b'/b), obtained by the present quasi-TEM analysis.

width (a'/a) and the normalized ridge height (b'/b). Suitable ridge loading provides a flat CN response over a broader range of frequencies, promising broadband operation of a TWT based on the ridge-loaded folded-waveguide SWS.

IV. Conclusion

A scheme for increasing the bandwidth of a TWT based on a serpentine folded-waveguide SWS by ridge loading has been presented and analyzed using a simple quasi-TEM approach including the effects of discontinuities due to both the folded-waveguide E-bend and the beam-holes. Unlike time-consuming 3-D electromagnetic analysis using CST Microwave Studio, the present analysis is simple and provides closed-form expressions for obtaining the dispersion and the interaction impedance characteristics of the structure. Such an analysis is quite useful as a design tool, particularly for rapid parametric studies in the early phases of the design. The explicit relationships between the design parameters provide physical insights into the dependence of the device performance on the structure parameters.

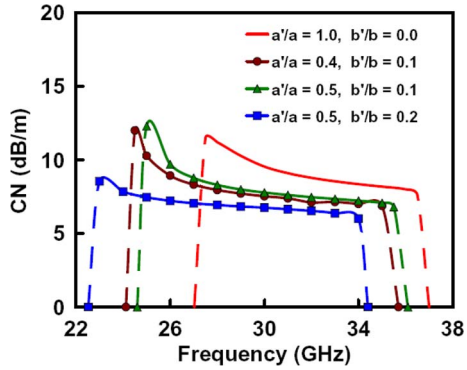

Fig. 8. Comparison of normalized circuit gain CN of the Ka-band structure for various combinations of ridge widths and ridge heights (with a beam voltage of 12 kV and a beam current of 120 mA).

The present quasi-TEM analysis is also convenient for analyzing a structure having multiple discontinuities, namely, inhomogeneous dielectric loading at selected locations, anisotropic ridge loading at selected locations, and ferrule loading around the beam holes. We plan to take up these aspects in future endeavors.

Appendix A
Approximate Parametric Analysis [4], [6]

An approximate yet very simple analysis for the dispersion relation of the SWS can be developed if one ignores the effects of the discontinuities due to the E-plane waveguide bend and the beam holes and considers that the TE_{10} mode pattern in the constituent ridged waveguide remains unaltered due to propagation in a serpentine path. Under these assumptions, the axial propagation constant may approximately be expressed following the parametric approach of Ha *et al.* [4] and Booske *et al.* [6] in the form

$$\beta_0 = \left(\frac{2\pi}{\lambda_g}\right)\left(1 + \frac{\lambda_g}{2l_{\text{eff}}}\right)\left(\frac{l_{\text{eff}}}{p}\right) \tag{A.1}$$

where l_{eff} $(= h + \pi(p - b + b')/2)$ is the effective path length of the RF wave per period. For the estimation of the interaction impedance, one has to use (9) but with the value of β_0 from (A.1).

Appendix B
Equivalent Circuit Analysis [7]

An equivalent circuit analysis was introduced by the present authors for a serpentine folded-waveguide SWS comprising conventional rectangular waveguide without ridge loading [7]. We modified the expressions of the lumped parameters of the beam holes following Collin [20] and that of the interaction impedance following Hutter [15], Liu [2], and Booske *et al.* [6].

The modified working expressions are presented here for the sake of validating the quasi-TEM and the parametric analyses, i.e.,

$$\beta_0 = \frac{1}{p}\left[2\pi - \cos^{-1}\left\{1 - (1/k)\left(1 - (f/f_W)^2\right)F_H\right\}\right]$$

$$K_c = Z_{PV}\left(\frac{1}{(\beta_0 p)}\left(\frac{\sin\{\beta_0 b/2\}}{\beta_0 b/2}\right)\right)^2$$

with

$$F_H = 2 + a_k - a_k(f/f_H)^2$$

$$f_W = \frac{1}{2\pi\sqrt{L_W C_W}} \qquad f_H = \frac{1}{2\pi\sqrt{L_H C_H}}$$

$$L_W = \frac{\mu_0 l_{\text{eff}} b}{\pi^2(l_{\text{eff}} + b)} \qquad C_W = \varepsilon_0 l_{\text{eff}}\frac{(l_{\text{eff}} + b)}{b}$$

$$L_H = \frac{1280\pi^2 r_c^3}{\omega\lambda_0 ab} \qquad C_H = \frac{r_c^3}{45\omega\lambda_0 ab}$$

$$k \approx 0.3\exp\{20 r_c/a\} \qquad a_k = \frac{L_H}{kL_W}.$$

For the case of no beam hole, $L_H = 0$, which makes $a_k = 0$ and $F_H = 2$. These formulas work within the parametric regime of $0 \le r_c/a \le 0.1$.

ACKNOWLEDGMENT

The authors would like to thank Dr. L. Kumar and Dr. K. S. Bhat for the constant encouragement and many valuable suggestions during the course of the work and Prof. B. N. Basu for a critical review of the manuscript and many valuable suggestions to improve this paper.

REFERENCES

[1] D. Gallagher, J. Richards, and C. Amstrong, "Millimeter-wave folded waveguide TWT development at Northrop Grumman," in *Proc. IEEE Int. Conf. Plasma Sci.*, 1997, p. 161.

[2] S. Liu, "Folded waveguide circuit for broadband MM wave TWTs," *Int. J. Infrared Millim. Waves*, vol. 16, no. 2, pp. 809–815, Feb. 1995.

[3] S. T. Han, J. Kim, and G. S. Park, "Design of folded waveguide traveling-wave tube," *Microw. Opt. Technol. Lett.*, vol. 38, no. 2, pp. 161–165, Jul. 2003.

[4] H. J. Ha, S. S. Jung, and G. S. Park, "Theoretical study for folded waveguide traveling wave tube," *Int. J. Infrared Millim. Waves*, vol. 19, no. 6, pp. 1229–1245, Sep. 1998.

[5] Y. H. Na, S. W. Chung, and J. J. Choi, "Analysis of a broadband Q band folded-waveguide traveling-wave tube," *IEEE Trans. Plasma Sci.*, vol. 30, no. 3, pp. 1017–1022, Jun. 2002.

[6] J. H. Booske, M. C. Converse, C. L. Kory, C. T. Chevalier, D. A. Gallagher, K. E. Kreischer, V. O. Heinen, and S. Bhattacharjee, "Accurate parametric modeling of folded waveguide circuits for millimeter-wave traveling wave tubes," *IEEE Trans. Electron Devices*, vol. 52, no. 5, pp. 685–693, May 2005.

[7] M. Sumathy, K. J. Vinoy, and S. K. Datta, "Equivalent circuit analysis of serpentine folded-waveguide slow-wave structures for millimeter-wave traveling-wave tubes," *Int. J. Infrared Millim. Waves*, vol. 30, no. 2, pp. 151–158, Feb. 2009.

[8] H. R. Yin, Y. Gong, Y. Wei, Z. Lu, M. Huang, and W. Wang, "Modified tunneladder slow-wave structures for high-power millimeter-wave TWTs," *Int. J. Infrared Millim. Waves*, vol. 28, no. 1, pp. 1–12, Jan. 2007.

[9] A. K. Ganguly, J. J. Choi, and C. M. Armstrong, "Linear theory of slow cyclotron interaction in double-ridged folded rectangular waveguide," *IEEE Trans. Plasma Sci.*, vol. 42, no. 2, pp. 348–355, Feb. 1995.

[10] R. C. Fletcher, "A broad-band interdigital circuits for use in traveling wave type amplifiers," in *Proc. IRE*, Aug. 1952, vol. 40, no. 8, pp. 951–958.

[11] J. C. Walling, "Interdigital and other slow wave structures," *J. Electron. Control*, vol. 3, pp. 239–258, Mar. 1957.

[12] F. Paschke, "A note on the dispersion of interdigital delay lines," *RCA Rev.*, vol. 19, no. 9, pp. 418–422, Sep. 1958.

[13] J. Hirano, "Characteristics of interdigital circuits and their use for amplifiers," in *Proc. Inst. Elect. Eng. Pt. B*, Dec. 1958, vol. 105, no. 12, pp. 780–785.

[14] J. Hirano, "A broad-band slow-wave structures for a millimeter traveling wave tube amplifiers," *IRE Trans. Electron Devices*, vol. ED-3, no. 3, pp. 228–234, Mar. 1962.

[15] R. G. E. Hutter, *Beam and Wave Electronics in Microwave Tubes*. New York: Van Nostrand, 1960.

[16] N. Marcuvitz, *Waveguide Handbook*. New York: McGraw-Hill, 1951.

[17] C. G. Montgomery, R. H. Dicke, and E. M. Purcell, *Principles of Microwave Circuits*. Stevenage, U.K.: IET, 1948, ser. MIT Radiation Series.

[18] S. Ramo, J. R. Whinnery, and T. Van Duzer, *Fields and Waves in Communication Electronics*. Singapore: Wiley, 1994.

[19] R. E. Collin, *Field Theory of Guided Waves*. New York: IEEE Press, 1991.

[20] R. E. Collin, *Foundations for Microwave Engineering*. New York: IEEE Press, 2001.

[21] S. B. Cohn, "Properties of ridge waveguide," in *Proc. IRE*, Aug. 1947, vol. 35, no. 8, pp. 783–788.

[22] T. S. Chen, "Calculation of the parameters of ridge waveguides," *IRE Trans. Microw. Theory Tech.*, vol. 5, no. 1, pp. 12–17, Jan. 1957.

[23] J. Helszajn, *Ridge Waveguide and Passive Microwave Components*. London, U.K.: IET, 2000.

[24] B. N. Basu, *Electromagnetic Theory and Applications in Beam-Wave Electronics*. Singapore: World Scientific, 1996.

M. Sumathy received the M.E. degree from the Department of Electronics and Communication Engineering, Madurai Kamaraj University, Madurai, India, in 1999. She is currently working toward the Ph.D. degree with the Indian Institute of Science, Bangalore, India.

She is currently a Scientist with the Microwave Tube Research and Development Centre, Defence Research and Development Organization (DRDO), Bangalore, India. Her research interests include slow-wave structures for traveling-wave tubes, high-power microwave (HPM) sources, and effects of HPM on electronic circuits.

Ms. Sumathy is a member of the Vacuum Electronic Devices and Applications Society (VEDAS), India. She received the DRDO Young Scientist Award in 2009.

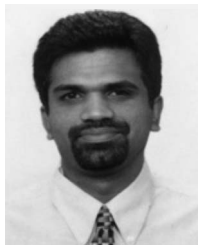

K. J. Vinoy (M'99) received the B.S. degree from the University of Kerala, Thiruvananthapuram, India, in 1990, the M.S. degree from Cochin University of Science and Technology, Cochin, India, in 1993, and the Ph.D. degree from the Pennsylvania State University, University Park, in 2002.

He was a Research Assistant with the Center for the Engineering of Electronic and Acoustic Materials and Devices, Pennsylvania State University, from 1999 to 2003. He is currently an Assistant Professor with the Department of Electrical Communication Engineering, Indian Institute of Science, Bangalore, India. He has published more than 50 papers in technical journals and conference proceedings. He is the author of the following books: *Radar Absorbing Materials: From Theory to Design and Characterization* (Boston: Kluwer, 1996) and *RF MEMS and their Applications* (London: John Wiley, 2002). He is the holder of one U.S. patent.

S. K. Datta (M'09) received the B.E. degree in electronics and telecommunication engineering from Bengal Engineering College, Calcutta University, Kolkata, India, in 1989 and the M.Tech. and Ph.D. degrees in microwave engineering from the Institute of Technology, Banaras Hindu University, Varanasi, India, in 1991 and 2000, respectively.

He is currently a Scientist with the Microwave Tube Research and Development Centre, Defence Research and Development Organization (DRDO), Bangalore, India. His current areas of research include computer-aided design and development of helix and coupled-cavity traveling-wave tubes, Eulerian and Lagrangian analysis of the nonlinear effects in traveling-wave tubes, and the studies on electromagnetic wave propagation in slow-wave structures.

Dr. Datta is a Fellow of the Institution of Electronics and Telecommunication Engineers of India and a member of Magnetics Society of India. He is the founding General Secretary and a Fellow of the Vacuum Electronic Devices and Applications Society (VEDAS), India. He received the Sir C. Ambashankaran Award of the Indian Vacuum Society for Best Paper in 1998, the INAE Young Engineer Award in 2001, the Sir C. V. Raman Young Scientist Award in 2002, the DRDO Agni Award for Excellence in Self Reliance in 2003, and the DRDO Laboratory Scientist of the Year Award in 2009.